Preparation and Properties of Polylactide–Silica Nanocomposites

Aiping Zhu, Huaxin Diao, Qianping Rong, Auyun Cai

College of Chemistry and Chemical Engineering, Yangzhou University, Yangzhou 225002, People's Republic of China

Received 21 April 2009; accepted 14 November 2009
DOI 10.1002/app.31786
Published online 28 January 2010 in Wiley InterScience (www.interscience.wiley.com).

ABSTRACT: Poly(lactic acid) (PLA)/SiO_2 nanocomposites were prepared via melt mixing with a Haake mixing method. To improve the dispersion of nanoparticles and endow compatibility between the polymer matrix and nanosilica, SiO_2 was surface-modified with oleic acid (OA). The interfacial adhesion of the PLA nanocomposites was characterized by field-emission scanning electron microscopy. The storage modulus and glass-transition temperature values of the prepared nanocomposites were measured by dynamic mechanical thermal analysis. The linear and nonlinear dynamic rheological properties of the PLA nanocomposites were measured with a parallel-plate rheometer. The effects of the filling content on the dispersability of the OA–SiO_2 nanoparticles in the PLA matrix, the interface adhesion, the thermomechanical properties, the rheological properties, and the mechanical properties were investigated. Moreover, the proper representation of the oscillatory viscometry results provided an alternative sensitive method to detect whether aggregation formed in the polymeric nanocomposites. © 2010 Wiley Periodicals, Inc. J Appl Polym Sci 116: 2866–2873, 2010

Key words: adhesion; composites; dispersions; nanocomposites

INTRODUCTION

The growth of environmental concern over nonbiodegradable, petrochemical-based plastic materials has raised interest in the use of biodegradable alternatives originating from renewable sources, such as aliphatic polyesters, including microbial polyesters, such as polyhydroxyvalerate and its copolymers (polyhydroxybutyrate–polyhydroxyvalerate), and chemically synthesized biopolymers, such as poly(glycolicacid), poly(ε-caprolactone), poly(vinyl alcohol), and poly(lactic acid) (PLA).[1–3]

Among aliphatic polyesters, PLA is one of most promising because it is thermoplastic, biodegradable, and biocompatible and has a high strength, a high modulus, and good processability.[3–7] In addition to its environmentally friendly nature, PLA can also be used for food contact surfaces and is generally recognized as safe. Because the production cost has been lowered by new technologies and large-scale production, the application of PLA has been extended to other commodity areas, such as packaging, textiles, composite materials,[6] and medical devices (for bone surgery, sutures, chemotherapy, etc.).[8,9]

In recent years, organic–inorganic nanocomposites with well-defined structures and morphology have become a very interesting and promising class of materials because of their potential use in a wide range of conventional application fields.[10–12] Particularly, silica-based organic–inorganic nanocomposites can be potentially used in many fields, such as plastics, rubbers, and coatings.[13–15] In polymer/silica nanocomposites, silica (hard fillers) can improve the strength, adhesion, durability, and abrasion resistance of polymeric materials. Thus, if silica nanoparticles are introduced into the PLA matrix, the aforementioned advantages are expected to be obtained. However, the compatibility and adhesion between silica and PLA are rather poor. The direct mixing of silica nanoparticles with PLA often leads to their aggregation within the PLA matrix and deterioration of the mechanical properties. To improve this situation, it is necessary to modify the silica particles. The most common method is the modification of the silica particles with a surfactant or with silane-coupling agents. Recently, Yan et al.[16] reported the surface modification of silica nanoparticles with a L-lactic acid oligomer by direct grafting onto the surface silanol groups (Si—OH) of the silica nanoparticles. The resulting toughness and tensile strength of the materials was greatly improved upon *g*-SiO_2 nanoparticle loading because of the good dispersion of nanosilica in the poly(L-lactic acid) matrix.

Correspondence to: A. Zhu (apzhu@yzu.edu.cn).

Contract grant sponsor: Jiangsu Province; contract grant numbers: SBK200930208 (Jiangsu Provincial Natural and Scientific Grant), SBC200910282 (Jiangsu Provincial Innovative Grant), 08KJA430003.

In this study, to improve embedding of nanofillers within the PLA matrix, oleic acid (OA) was used to surface-modify the nanosilica. The obtained OA–silica nanoparticles were then used as fillers in PLA to prepare its nanocomposites. The effects of filling content on the performance of the PLA nanocomposites were investigated.

EXPERIMENTAL

Materials

PLA (Biomer L9000, weight-average molecular weight = 200 kDa, weight-average molecular weight/number-average molecular weight = 1.98) was obtained from Biomer, Inc. (Krailling, Germany). The PLA resins were dried in a vacuum oven at 60°C for 24 h before use. OA was provided by Shanghai Chemical Reagent Co., Ltd. (Shanghai, China). Fumed silica was donated by Nanjing University of Technology (Nanjing, China) and had an average diameter of 25 nm. The particles were dried at 120°C *in vacuo* for 24 h to eliminate physically adsorbed and weakly chemically adsorbed species. All other reagents were analytical grade and were used without further purification.

Modification of the nanosilica by OA

Fumed silica (6.3 g) was first dispersed for 3 h in 90 mL of distilled water with the aid of an ultrasound bath. Then, 1.5 mL of OA was added to the dispersion, and this mixture was vigorously stirred for 90 min at room temperature with a magnetic stirrer. Afterward, 5 mL of a 25 wt % aqueous ammonia solution was added to the solution, and the agitation was continued overnight. Then, the dispersion was neutralized with a 30 wt % aqueous HCl solution. The mixture was centrifuged (2500 rpm) for 30 min, and the obtained precipitates were washed three times with 15 mL of a 1/1 ethanol/water (V/V) solution to remove excess OA. The resulting precipitates were dried in an oven at 50°C for 24 h to yield 4.5 g of modified nanosilica powder.

Preparation of the sheets

For the preparation of the thermocompressed films, PLA was thermally compacted with a Carver laboratory press (model 3925 hydraulic unit, Carver, Inc., Wabash, IN). About 2 g of PLA was placed between two stainless steel plates (1 mm thick, 25.4 cm wide, and 25.4 cm long) lined with aluminum foil, and then were inserted between the platens of the press and were heated to 190°C. A pressure of about 10,000 psi (68.9 MPa) was applied for 3 min, and this was followed by the removal of the aluminum foil liners, which were still attached to the compacted PLA film from the stainless steel plates. The PLA film layer was easily peeled from the aluminum foil layers after they were cooled in air to room temperature.

Rheological properties

The rheological properties were studied with a Rheometric Scientific (Waltham, MA) advanced research-grade rheometer with a parallel-plate geometry with a diameter of 25 mm. The compression-molded samples (12 g PLA and its composite particles), stacked to a thickness of about 0.9 mm, were investigated at 170°C (in the molten state). The following tests were performed: (1) a dynamic strain sweep to assess the deformation amplitude from the region of linear viscoelastic response at 10 rad/s, (2) a dynamic frequency time sweep to detect the stability of the sample behavior at 10 rad/s; and (3) a dynamic frequency sweep over an angular frequency range starting from a high of 100 Hz down to 0.01 Hz to expose the samples to a shorter thermal loading. The samples were placed between hot plates and stabilized at an experimental temperature of 170°C for about 5 min before the measurement. For each experiment, a new sample was taken. The experimental data were related to the actual gap value.

Characterization

Fourier transform infrared (FTIR) spectroscopy was applied to characterize the changes in the chemical structure of the silica after surface modification. Thin film specimens were pressed with KBr powder. Thermogravimetric analysis (TGA) measurements were performed on a Netzsch STA 409PC thermogravimetric analyzer (Selb, Bavaria, Germany) from 25 to 600°C at a heating rate of 10°C/min under a flow of anhydrous air. The morphologies of the fracture surfaces were observed by field-emission scanning electron microscopy (FESEM; S-2150, Hitachi). The specimens were fractured after immersion in liquid nitrogen. The fractured surfaces of the specimen were coated with a thin layer (10–20 nm) of gold and palladium before SEM examination. The dynamic thermomechanical properties of the nanocomposites were measured with a Rheometric Scientific analyzer (DMA 242C, Netzsch). The bending (dual-cantilever) method was used with a frequency of 1 Hz and a strain level of 0.04% in the temperature range f 25–90°C. The heating rate was 3°C/min. The testing was performed with rectangular bars measuring approximately $30 \times 10 \times 3$ mm^3. These were prepared with a hydraulic press at a temperature of 180°C and a pressure of 100 bar for a time

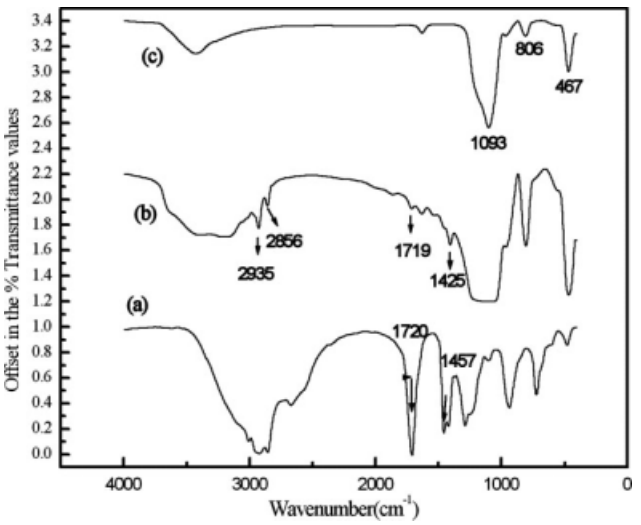

Figure 1 FTIR spectra of (a) OA, (b) OA–SiO_2, and (c) SiO_2.

period of 5 min. The exact dimensions of each sample were measured before the scan. The tensile properties of the nanocomposites were determined with an AG-2000 universal material testing machine (Shanghai Hua Long Test Instrument Factory, Shanghai, China) at a crosshead speed of 50 mm/mm according to the national standard GB1040-79. All of the mechanical tests were carried out at 25°C. The melting behaviors of the PLA nanocomposites were tested in a 204 F1 differential scanning calorimeter from Netzsch Gerateban GmbH Instruments. Samples of 5 ± 0.01 mg were used. Melting was performed at heating rate of 10°C/min. The crystallinity of the samples was determined from the heat of melting.

RESULTS AND DISCUSSION

Characterization of the OA-modified SiO_2 nanoparticles

Ding et al.[17] used OA for the first time as a functionalized monomer. They reported that OA could bond to the silica surface with a single hydrogen bond. To separate the unbonded OA, the silica nanoparticles were extracted with acetone in a Soxhlet apparatus for 24 h. Figure 1 shows the FTIR spectrum of OA, SiO_2, and OA–SiO_2. As shown in the spectrum of OA–SiO_2, there was a very pronounced band appearing at 1093 cm^{-1}, together with two less pronounced bands at 806 and 467 cm^{-1}, corresponding to the vibration absorption of Si—O—Si groups. The peaks at 2935, 2856, and 1415 cm^{-1} were associated with the characteristic vibration of carbohydrate, and the peak at 1719 cm^{-1} corresponded to the vibration absorption of carbonyl groups (C=O). These results suggest that OA was successfully incorporated onto the surface of SiO_2.

Figure 2 illustrates the TGA thermogram of OA–SiO_2. The weight loss before 100°C was caused by the adsorbed water in the nanoparticles. The content of OA bonded on the SiO_2 was measured from the residue weight ratio of the OA–SiO_2. The weight loss for OA was determined to be about 9 wt %, which indicated that about 9 wt % OA was incorporated onto the SiO_2.

PLA nanocomposites

Morphology

It was necessary to study the morphology of the polymer composites because their mechanical properties depended on it. FESEM micrographs of PLA and its composites are presented in Figure 3. As shown, the edges and corners of virgin PLA were very smooth [Fig. 3(a)]; this demonstrated obvious brittle rupture. In the PLA nanocomposites, the fracture morphology was strongly dependent on the filling content of OA–SiO_2. As shown in Figure 3(b), the spherical particles were well dispersed in the PLA nanocomposite filled with 1 wt % OA–SiO_2. Moreover, the interface between the inorganic and polymeric phases became rougher than that of virgin PLA. The interface was the roughest and most adhesive for the PLA nanocomposites filled with 3 wt % OA–SiO_2 [Fig. 3(c)].

Dynamic mechanical thermal properties

Dynamic mechanical thermal analysis (DMTA) is a reliable approach for the examination of the relaxation behavior of materials. To evaluate the effect of the OA–SiO_2 filling, the thermomechanical properties were measured. The mechanical relaxation data of the PLA composites [loss tangent (tan δ) and storage modulus (E')] are depicted in Figure 4(a,b). Tan δ for all of the composites reached a maximum

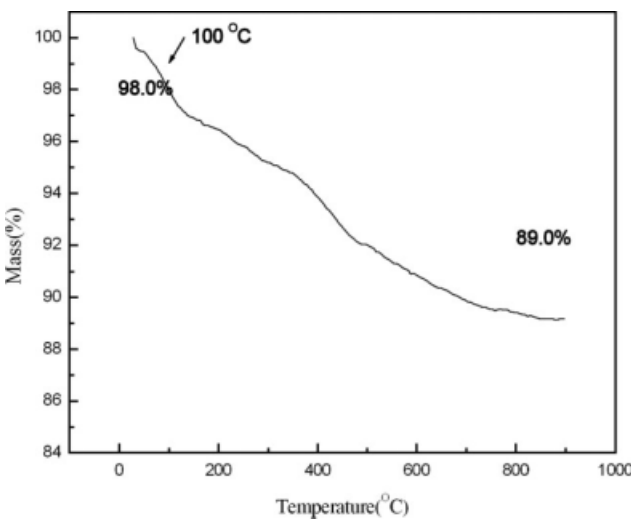

Figure 2 TGA of OA–SiO_2.

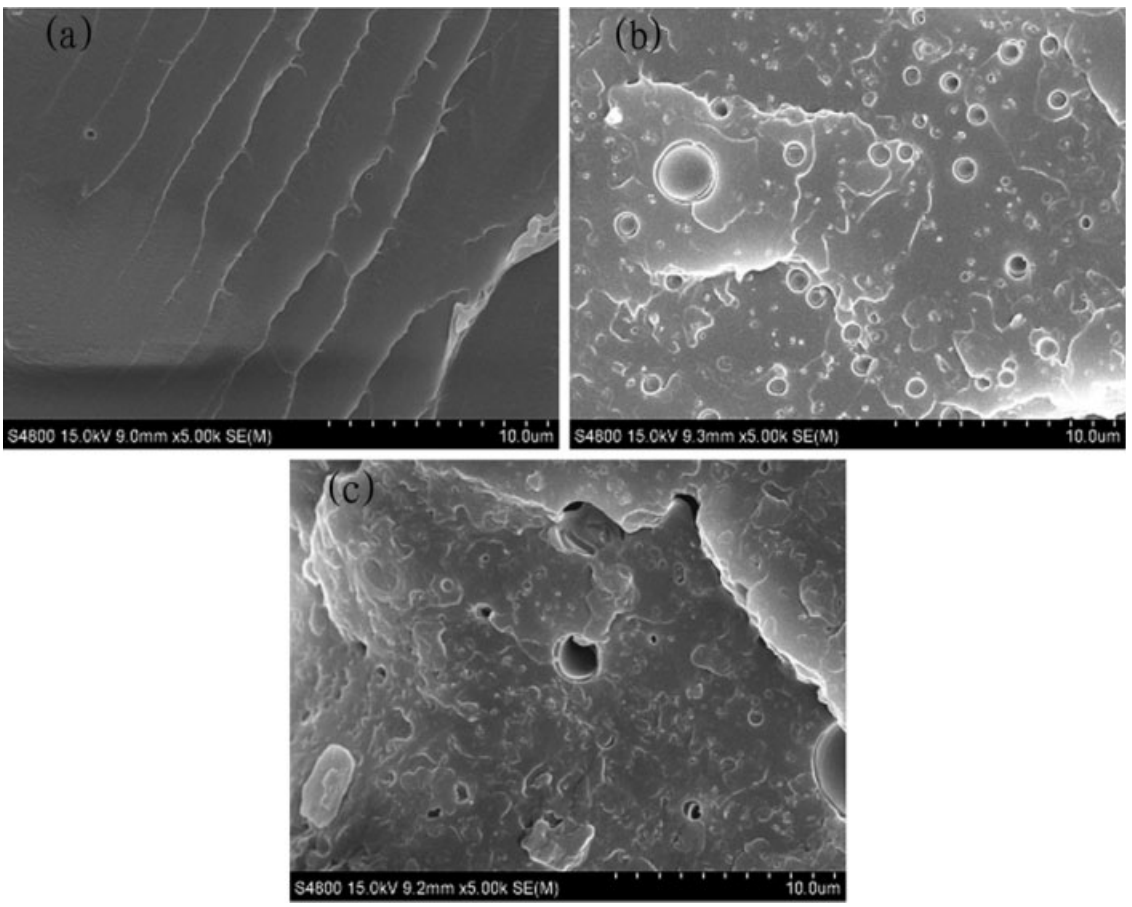

Figure 3 FESEM fractures of PLA and its nanocomposites: (a) PLA, (b) PLA filled with 1 wt % OA–SiO_2, and (c) PLA filled with 3 wt % OA–SiO_2.

in the temperature range 60–70°C; this relaxation corresponded to the glass-transition temperature (T_g) of PLA. As shown in Figure 4(a), T_g of the PLA composites was lower than that of virgin PLA, and T_g decreased with increasing filling content of OA–SiO_2. In general, T_g of a polymeric composite tends to increase with nanoscale filler content because of the interaction between the polymer and the nanoscale filler. Herein, the decrease in T_g was thought to be likely associated with the plastication of OA–SiO_2 nanoparticles on the PLA chains. Moreover, Figure 4(b) indicates that the PLA nanocomposite had a lower E' than virgin PLA. At first, with the addition of OA–SiO_2, E' decreased significantly to a 1 wt % filling content. Afterward, when the nanocomposite was filled with 3 wt % OA–SiO_2, E' increased near to the level of PLA. When the filler content was increased further to 5 wt %, E' decreased again, which may have been caused by the aggregation of OA–SiO_2 in the PLA matrix; this weakened the effect of the nanofillers. For composite systems, it is well known that filling with a spherical mineral filler will increase E' because of the rigidity of the fillers. These results suggest that OA–SiO_2 had adverse effects on E'. On one hand, plastication led to decreased T_g and E' values; on the other hand, the rigidity of OA–SiO_2 was in favor of increasing E'.

Crystallization behavior

Differential scanning calorimetry (DSC) was used to study the thermal properties of PLA and its nanocomposites. Data for the melting endotherm as a function of temperature is shown in Figure 5. The melting enthalpy (ΔH_m) and the melting temperature (T_m) obtained from Figure 5 are listed in Table I. T_m of the PLA composite shifted to a lower temperature compared to that of PLA. ΔH_m for pure PLA was 9.3 J/g, whereas for the PLA nanocomposite filled with 0.5 wt % OA–SiO_2, it was 6.9 J/g. The decreased ΔH_m value of the PLA nanocomposite filled with 0.5 wt % OA–SiO_2 was probably due to the fact that a low concentration of nanosilica could form strong interactions with PLA, which prohibited the movement of the polymer segments and caused the polymer chain arrangement to become more difficult; this disrupted the regularity of the PLA chain structures. In the PLA nanocomposites filled more than 0.5 wt % OA–SiO_2 nanoparticles, ΔH_m

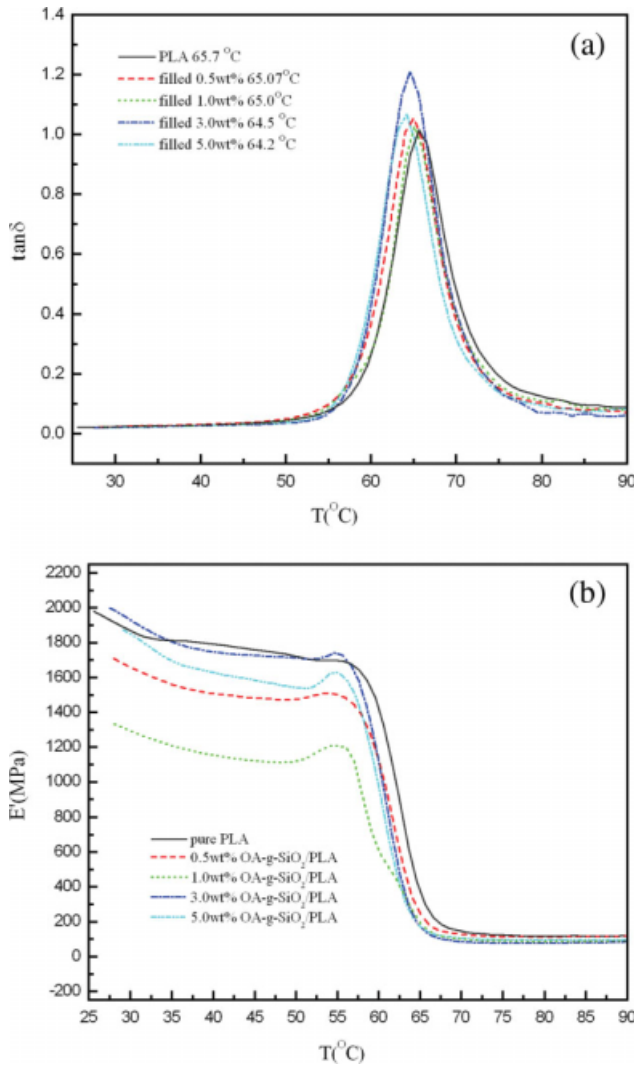

Figure 4 DMTA of PLA and its composites: the dependence of (a) tan δ and (b) E' on temperature (T). [Color figure can be viewed in the online issue, which is available at www.interscience.wiley.com.]

increased compared with that of virgin PLA. The increase in ΔH_m indicated that the higher concentration of OA–SiO_2 nanoparticles promoted PLA crystallization because ΔH_m could be used as an indication of percentage crystallinity of PLA. The DSC results suggest that when the filling content was greater than 0.5 wt %, the OA–SiO_2 nanoparticles showed a distinguished nucleating effect. However, the use of a low concentration of OA–SiO_2 nanoparticles (e.g., 0.5 wt %) demonstrated obvious crystal destruction.

Rheological properties

The variation of steady-state viscosity as a function of the shear rate is presented in Figure 6. It was evident that the viscosity of the PLA nanocomposite filled with 0.5 wt % OA–SiO_2 was at a minimum. This was because that low concentration of OA–SiO_2

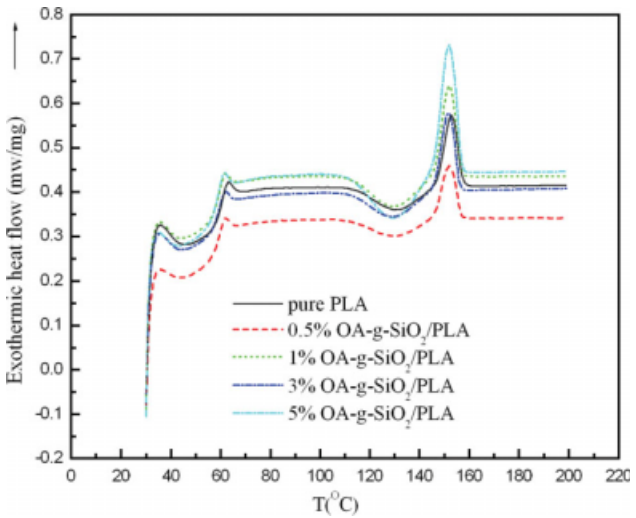

Figure 5 DSC thermograms of melting for PLA and its nanocomposites (T = temperature). [Color figure can be viewed in the online issue, which is available at www.interscience.wiley.com.]

nanoparticles disrupted the regularity of the PLA chain structures and increased the space between the chains and promoted the mobility of the chain segments in the direction of flow. The viscosity of the PLA nanocomposites increased with increasing filling content. For the PLA nanocomposite filled with 3 wt % OA–SiO_2 nanoparticles, the viscosity became higher than that of virgin PLA. This was because the higher concentration of nanosilicas perturbed the normal flow of the PLA and hindered the mobility of the chain segments in the direction of flow. With further increases in the filling amount, the viscosity did not increase accordingly.

The typical linear viscoelastic behavior of PLA and its nanocomposites is shown in Figure 7. This figure indicates that the linear region of the PLA filled with 5 wt % OA–SiO_2 was much narrower than that of virgin PLA and the other PLA nanocomposites. This result suggests that the higher concentration of OA–SiO_2 filling leads to the agglomeration of nanoparticles and deaggregation under certain stress.

The frequency-dependent elastic modulus of PLA and its nanocomposites is presented in Figure 8. The

TABLE I
T_m and ΔH_m Values of PLA and Its Nanocomposites Obtained from DSC Analysis

Sample	T_m (°C)	ΔH_m (J/g)
PLA	152.9	9.3
0.5 wt % OA–SiO_2/PLA	152.0	6.9
1 wt % OA–SiO_2/PLA	152.0	12.2
3 wt % OA–SiO_2/PLA	151.8	10.3
5 wt % OA–SiO_2/PLA	152.0	18.4

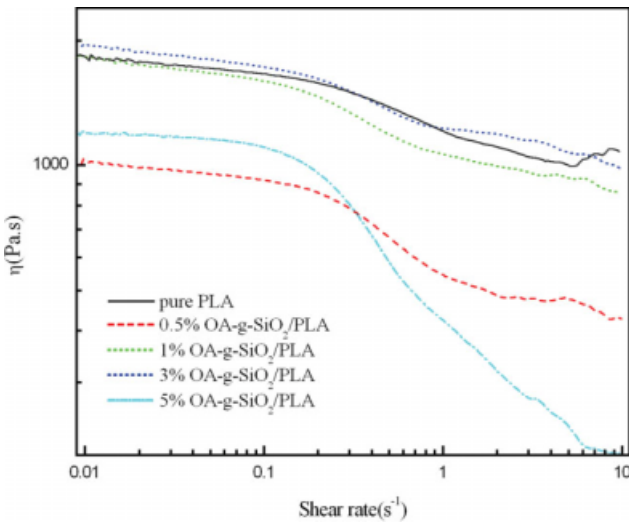

Figure 6 Effect of OA–SiO_2 filling content on the steady-state viscosity (η). [Color figure can be viewed in the online issue, which is available at www.interscience.wiley.com.]

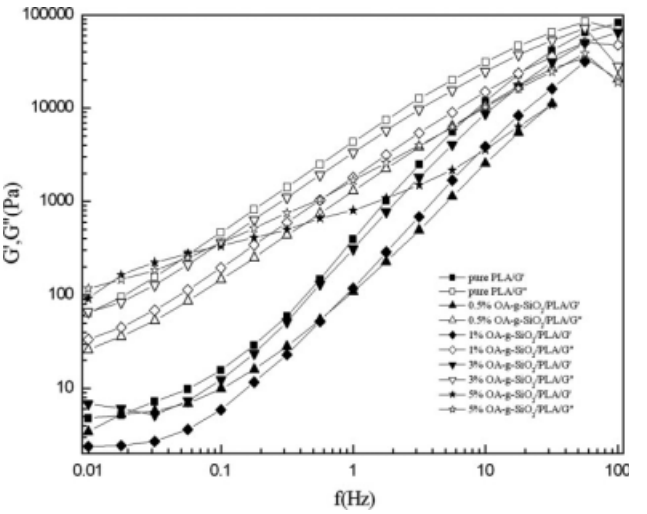

Figure 8 Frequency (*f*)-dependent elastic modulus of PLA and its nanocomposites.

elastic modulus of the PLA nanocomposites filled a low concentration of OA–SiO_2 nanoparticles (e.g., 0.5 and 1.0 wt %) decreased significantly in comparison with that of virgin PLA, which indicated obvious plastication of the OA–SiO_2 nanoparticles in these nanocomposites. The elastic modulus of the PLA nanocomposite filled with 3.0 wt % OA–SiO_2 nanoparticles was little lower than that of virgin PLA. The elastic modulus curves (except that of the PLA nanocomposite filled 5 wt % OA–SiO_2) implied that large-amplitude shear induced an oriented structure in these nanocomposites. Furthermore, these curves were almost parallel with each other in the whole frequency region, and no plateau was observed in these systems. The lack of a plateau in the frequency-dependent curve reflected the relatively weak interactions between the nanoparticles and the uniform distribution of nanoparticles in the PLA matrix. However, the elastic modulus curve for the PLA nanocomposite filled with 5 wt % OA–SiO_2 nanoparticles demonstrated a great difference from the others. First, the storage modulus (G') was almost independent of the frequency in the range of low frequency (<0.1 Hz); this was indicative of a transition from liquidlike to solidlike viscoelastic behavior. Therefore, we concluded that a filler–network structure formed in the PLA nanocomposite.

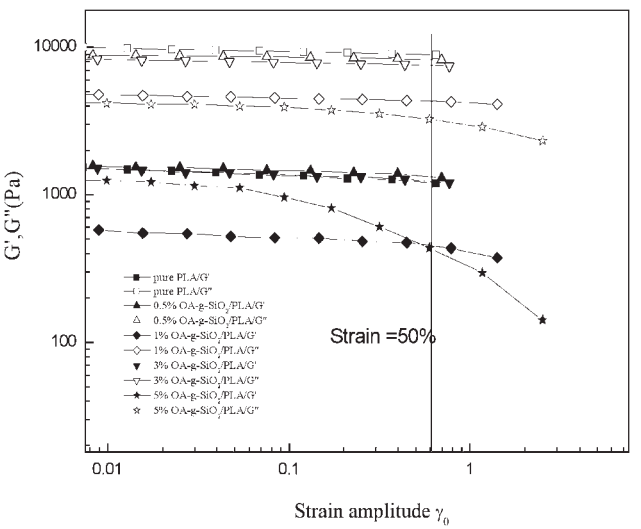

Figure 7 Typical linear viscoelastic behavior of PLA and its nanocomposites at 190°C (angular frequency = 100 rad/s).

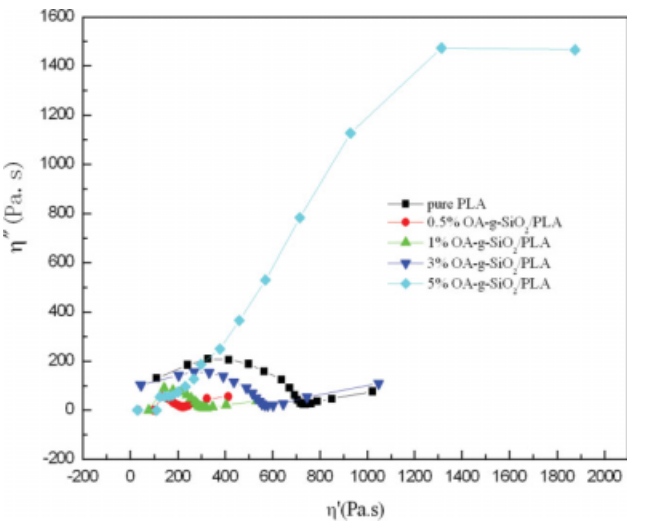

Figure 9 Cole–Cole representation of the dynamic viscosity of PLA and its nanocomposites. η′, dynamic viscosity; η″, storage viscosity. [Color figure can be viewed in the online issue, which is available at www. interscience.wiley.com.]

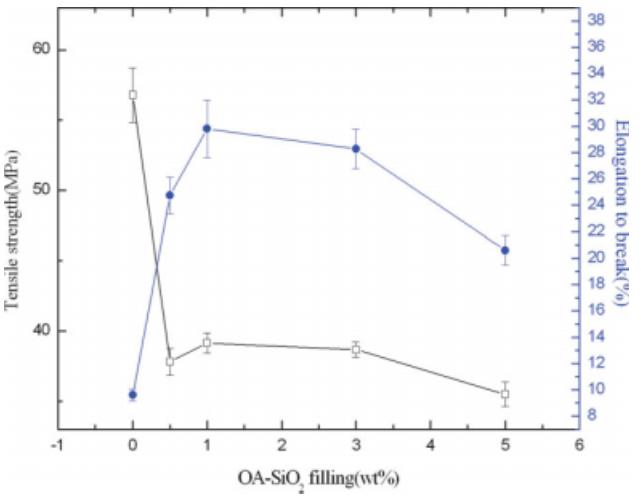

Figure 10 Mechanical properties of PLA and its nanocomposites. [Color figure can be viewed in the online issue, which is available at www.interscience.wiley.com.]

Second, a point of intersection appeared in the G' and loss modulus (G'') curves. In the low-frequency range, G' was higher than G'', whereas in the high-frequency range, G'' was higher than G'. These results verified the filler–network structure formed in this PLA nanocomposite.

Rheology is often used for the characterization of polymer melts and for the detection of various structures in them. The formation of aggregates might be detected by dynamic viscometry, the measurement of the complex viscosity, and other linear viscoelastic characteristics of the melt as a function of frequency.[18,19] Cole–Cole plotting was shown to very sensitively detect the formation of higher order structures in polymer melts.[19,20] In this presentation, the imaginary part is plotted against the real part of a complex elastic property. The plot should be a perfect arc if higher order structures are absent, and the relaxation behavior of the melt can be described by a single relaxation time.[20,21] A broad relaxation time spectrum leads to the flattening of the arc, whereas structure effects result in the appearance of a second arc, a tail, or an increasing correlation.[19] The dynamic viscosities of PLA and its nanocomposites are plotted in this way in Figure 9. The Cole–Cole plots were arclike for PLA and its nanocomposites (expect for the composite filled with 5 wt % OA–SiO_2). The Cole–Cole plot for the PLA nanocomposite filled with 5 wt % OA–SiO_2 was not an arc; this suggested that a higher order structure (a filler–network structure) was present in this composite. Rheology has been verified to be a very sensitive tool for detecting whether aggregation forms in a polymeric nanocomposite.

Mechanical properties

Figure 10 shows the tensile strength at break and the elongation at break versus the OA–SiO_2 nanoparticle filling content. The tensile strength at break decreased markedly with OA–SiO_2 nanoparticle filling content. However, the elongation at break increased significantly with the addition of OA–SiO_2 nanoparticles in comparison with that of virgin PLA (9.4%). The elongation at break increased with increasing filling content up to 1 wt % OA–SiO_2 nanoparticles (29.8%, 3.2 times than that of virgin PLA); afterward, the elongation at break started to decrease with further increases in the filling content. This was because the mechanical properties strongly depended on the dispersion and phase size of nanosilica in the polymer matrix. These results demonstrate that the OA–SiO_2 nanoparticles were effective fillers for improving the flexibility of PLA because a suitable filling content was as low as 1 wt %.

CONCLUSIONS

In this study, to improve the compatibility between inorganic SiO_2 and PLA, OA was used to surface-modify nanosilica. The obtained OA–SiO_2 nanoparticles were used to fill PLA to prepare its nanocomposites. Fractography revealed the good dispersability of the OA–SiO_2 nanoparticles in the PLA matrix and the better interfacial adhesion in the PLA nanocomposites compared to that of unfilled PLA. A low concentration of OA–SiO_2 nanoparticles (<1 wt %) showed obvious plastication. The rheological properties of the PLA nanocomposites were dependent on the OA–SiO_2 filling content. Proper representation of the oscillatory viscometry result allowed us to detect whether aggregation formed in the PLA nanocomposites. OA–SiO_2 nanoparticles were found to be effective fillers for improving the flexibility of PLA.

References

1. Briassoulis, D. J Polym Environ 2004, 12, 65.
2. Chandra, R.; Rustgi, R. Prog Polym Sci 1998, 23, 1273.
3. Lenz, R. W.; Marchessault, R. H. Biomacromolecules 2005, 6, 1.
4. Tsuji, H.; Ikada, Y. J Appl Polym Sci 1998, 67, 405.
5. Lunt, J. Polym Degrad Stab 1998, 59, 145.
6. Drumright, R. E.; Gruber, P. R.; Henton, D. E. Adv Mater 2000, 12, 1841.
7. Hakkarainen, M. Adv Polym Sci 2002, 157, 113.
8. Mikos, A. G.; Lyman, M. D.; Freed, L. E.; Langer, R. Biomaterials 1994, 15, 55.
9. Park, T. G.; Cohen, S.; Langer, R. Macromolecules 1992, 25, 116.
10. Castelvetro, V.; Vita, C. D. Adv Colloid Interface Sci 2004, 108, 167.

11. Ray, S. S.; Okamoto, M. Macromol Rapid Commun 2003, 24, 815.
12. Paul, M. A.; Alexandre, M.; Degee, P.; Henrist, C.; Rulmont, A.; Dubois, P. Polymer 2003, 44, 443.
13. Kasiwagi, T.; Morgan, A. B.; Antonucci, J. M.; Van Landingham, M. R.; Harris, R. H., Jr.; Awad, W. H.; Shields, J. R. J Appl Polym Sci 2003, 89, 2072.
14. Peng, Z.; Kong, L. X.; Li, S. D.; Chen, Y.; Huang, M. F. Compos Sci Technol 2007, 67, 3130.
15. Mammeri, F.; Rozes, L.; Bourhis, E. L.; Sanchez, C. J Eur Ceram Soc 2006, 26, 267.
16. Yan, S. F.; Yin, J. B.; Yang, Y.; Dai, Z. Z.; Ma, J.; Chen, X. S. Polymer 2007, 48, 1688.
17. Ding, X. F.; Zhao, J. Z.; Liu, Y. H.; Zhang, H. B.; Wang, Z. C. Mater Lett 2004, 58, 3126.
18. Lertwimolnun, W.; Vergnes, B. Polymer 2005, 46, 3462.
19. Abranyi, A.; Szazdi, L.; Pukanszky, B., Jr.; Vancso, G. J.; Pukanszky, B. Macromol Rapid Commun 2006, 27, 132.
20. Deby, P. Polar Molecules; Chemical Catalogue: New York, 1929.
21. Cole, K. S.; Cole, R. H. J Chem Phys 1941, 9, 341.